Modeling Three-Point Bending of Rock-Type Materials Using an Elastoplastic Model with Contact Elements

S. K. Kourkoulis[1], Z. Agioutantis[2], S. Maurigiannakis[2], and E. Papatheodorou[2]

[1]*National Technical University of Athens, Department of Mechanics*
Zografou Campus, Theocaris Building, 157 73 Zografou, Athens, HELLAS
email: stakkour@central.ntua.tuc.gr
[2]*Technical University of Crete, Department of Mineral Resources Engineering,*
731 00 Hania, Crete, HELLAS
email: zach@mred.tuc.gr

1. SUMMARY

The three-point bending (3PB) test of prismatic beams made from shellstone is studied both numerically and experimentally. The numerical study is carried out using a 2D Finite Element Analysis. The shellstone is modeled as a linearly elastic-ideally plastic material obeying a parabolic Mohr-Coulomb failure law. The numerical results are in satisfactory agreement with experimental values from 3PB tests.

2. INTRODUCTION

The calculation of the stress and strain fields in a relatively short prismatic beam under the action of a transverse concentrated load is a difficult task and a closed form solution does not exist yet. Relative studies have already been reported since the end of the 19th century. The pioneering experimental works by Wilson /1/ and Flamant /2/ and the analytical models by Boussinesq /3/ and Filon /4/ are among the earlier ones. Later the problem was revisited by Carman /5/, Seewald /6/, Timoshenko /7/ and others. However, even today the problem has not been solved analytically and the determination of the stress and strain fields remains the subject of extensive experimental and numerical work. The problem is more complicated in the case where the beam material cannot be considered as linearly elastic and isotropic. A general solution of the problem is not available, even for the relatively simple cases of linearly elastic-ideally plastic or of transversely isotropic soft rocks. However, such materials are widely used, among others, for the restoration of important monuments made from porous stones and shellstones. Thus an in-depth investigation of such problems appears to be indispensable.

In order to overcome these difficulties the problem is studied here numerically with the aid of the Finite Element Method. Attention is focused on the material used by ancient Greeks for the erection of the Zeus Temple at Olympia, a type of soft rock called conchyliates (shellstone). As a first step it is assumed that plane strain conditions prevail, and the complicated constitutive relationship of the material is modeled as linearly elastic-ideally plastic. The results of the numerical analysis are then compared with those obtained from a series of 3PB tests with prismatic specimens prepared from freshly quarried shellstone.

3. EXPERIMENTAL PROCEDURE

The material

The specimens for the experiments were made from shellstone quarried from the wider Olympia site. It is an inhomogeneous material, of layered structure consisting of successive layers of seashells, bonded relatively loosely to each other with the aid of carbonate material. The size of the shells exhibits very strong variation between some millimeters and a few centimeters. The thickness of the layers is of the order of a few millimeters. This structure imposes a transversely isotropic character to the material with two distinct axes of anisotropy: one perpendicular to the material layers and one within their plane. The mechanical behaviour of such materials is described with the aid of five material constants.

Typical stress-strain curves of shellstone under uniaxial compression are shown in Fig.1 /8/. These experiments show that up to the peak load the constitutive law is almost linearly elastic. Then an abrupt load drop is observed leading to the post peak regime, which is characterized by a very small slope almost up to the final disintegration of the specimens. It should also be noted that two different failure mechanisms were activated. Specimens made from recently excavated material fail due to the formation of cracks oriented almost parallel to the axis of the load. In this case the finally recorded strain is relatively low. On the other hand, for specimens cut from ancient material, the formation of cracks parallel to the load is followed by a stage of gradual collapse of successive horizontal shell layers under almost constant overall load. The finally recorded strain in this case is relatively high, of the order of about 4%.

The three-point bending tests

A series of 3PB tests was carried out with prismatic specimens 42 cm long and 10x10 cm in cross-section. They were placed on two steel rollers (diameter 2 cm) at a distance of 40 cm from each other. The load was applied uniformly along the thickness of the specimens with the aid of a third identical steel roller. The strains developed were measured using electrical strain gauges positioned according to a cartesian reference system at the intersections of three vertical (x=0, -5, -10 cm) and five horizontal (y=-4.5, -2.5, 0, 2.5, 4.5 cm) lines (Fig.2). Also, three dial-gauges of sensitivity 10^{-5} m were placed at points (x,y)=(0cm,5cm), (-5cm, 5cm), (-10cm,5cm) for the measurement of the deflections of the beam.

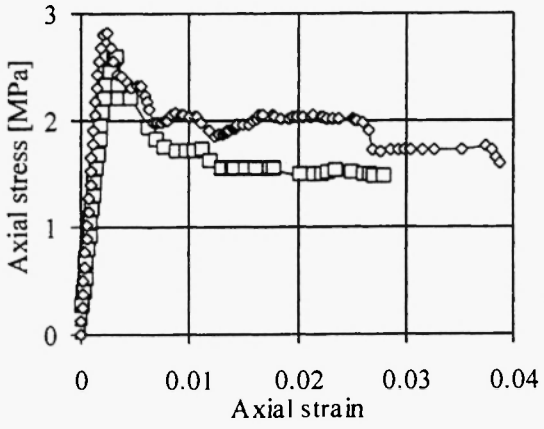

Fig.1: The axial stress-axial strain diagram of the shellstone of the tests /8/.

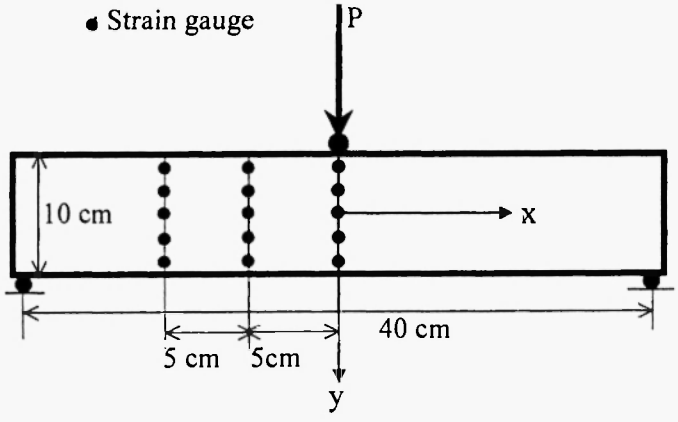

Fig. 2: Schematic configuration of the specimens and the position of the strain gauges.

The specimens were cut parallel to the material layers. The longitudinal axis of the beams was oriented parallel to the material layers, while the y-axis of the reference system (Fig. 2) was normal to them. The load was applied statically at a constant displacement rate of 3x10^-3 cm/min with the aid of a stiff hydraulic frame of capacity 250 kN. Taking into account that the maximum load recorded during the whole series of 3PB tests did not exceed 3.5 kN in any case, the stiffness of the frame can be considered infinite.

Typical experimental results for the deflection of the beam just before fracture are shown in Fig. 3, while in Fig. 4 the deflection of the lowest point of the central section is plotted vs. the external load. In both cases the experimental results agree well with the numerical ones (continuous lines), although some discrepancies appear especially for the deflection of the mid-section for loads approaching the fracture load.

4. NUMERICAL SOLUTION AND RESULTS

Geometry

The test was modeled in 2-d space in the MSC.Mentat front-end program, and was solved by the MSC. Marc Finite Element Analysis program /9,10/. To fully simulate the behavior of the materials during bending, both the rock and the steel cylinders used to apply the load were modeled. Contact elements were introduced to model the interface between steel and rock. Symmetry was not taken into consideration and thus the dimensions of the final model matched those of the experimental set up (Fig. 5). The model consisted of 1246 plane strain elements and 1167 nodes. Node positions were defined to coincide with strain measuring points on the specimen. Figs. 6 and 7 show in detail the contact area between steel and rock.

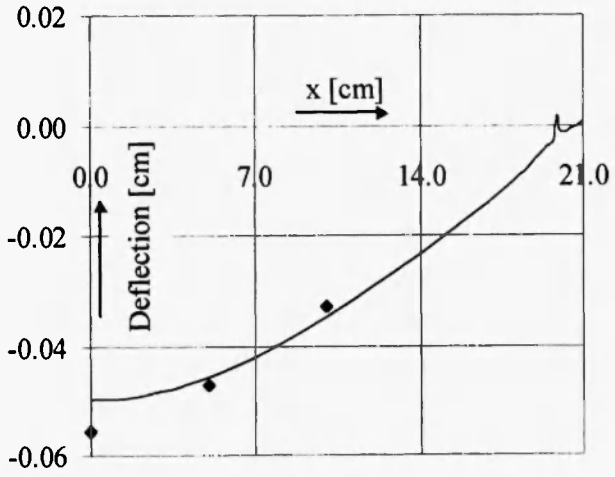

Fig. 3: The deflection of the lowest side of the beam just before fracture.

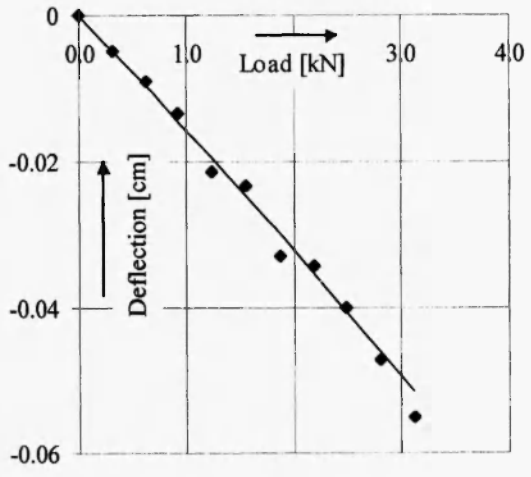

Fig. 4: The deflection of the mid-section of the beam versus the external load.

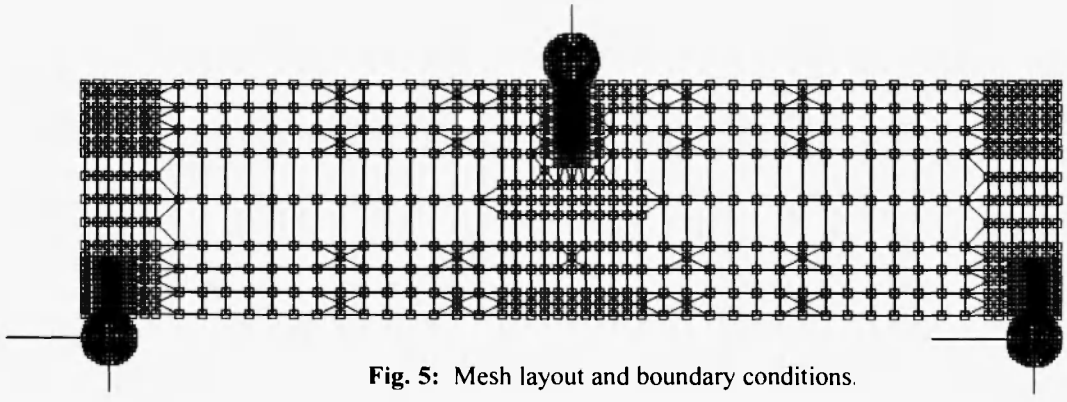

Fig. 5: Mesh layout and boundary conditions.

Material models and boundary conditions

Steel was modeled as an elastic material of elastic modulus E=210 GPa and Poisson's ratio v=0.3. The respective values for the shellstone were E=1.1 GPa and v=0.25. The shellstone was modeled as an elastoplastic material using a parabolic Mohr-Coulomb failure criterion. Its parameters were obtained through calibration testing as: $\sigma = 0.265$ MPa and $\beta = 0.0757$ for the following yield condition:

$$f = \left(3J_2 + \sqrt{3}\beta\bar{\sigma}J_1\right)^{1/2} - \bar{\sigma} = 0, \quad \sigma^2 = 3[c^2 - (\alpha^2/3)], \quad \beta = \alpha/[3(3c^2 - \alpha^2)]^{-1/2} \tag{1}$$

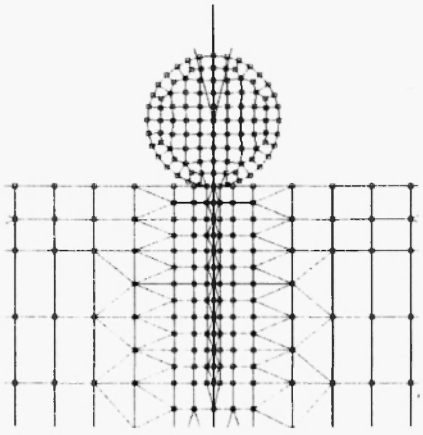

Fig. 6: Detailed view of the steel-shellstone contact.

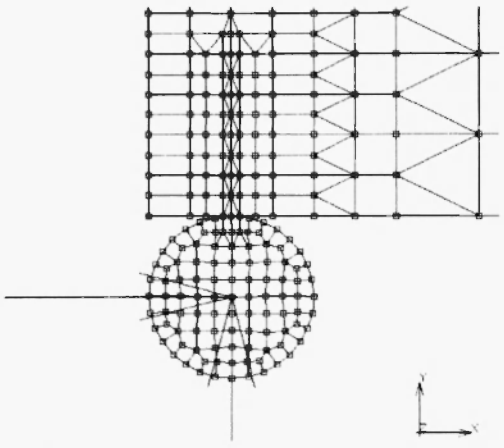

Fig.7: Detailed view of the supporting cylinder.

Contact elements were introduced between the shellstone specimens and the steel cylinders. However, in all contact cases there were three common nodes between the steel cylinders and the rock. The friction coefficient between shellstone and steel was set to 0.4 /11/. A maximum load of 3.125 kN was applied on the central cylinder in ten steps (Fig.6). The centers of the bottom cylinders were fixed for both horizontal and vertical displacements (Fig.7). No other boundary conditions were required (Fig.5).

Results of the numerical study

For every load step, displacements, stresses and strains were calculated at each node. The distribution of axial and transverse strains along the bottom line of the specimen, i.e. the line with y=5 cm, is plotted in Fig.8, while Fig.9 presents the variation of the components of the stress tensor along the same line. It is clear from these figures that the distributions are qualitatively similar to those predicted by the Bernoulli-Euler theory, since the transverse and shear stresses are negligible compared to the respective axial ones. The only exception is the immediate vicinity of the supporting cylinders where the concentrated reaction forces generate considerable transverse stresses, exceeding in magnitude the axial ones. The situation, however, is completely different as one moves towards the load application point. In Figs.10&11 the strain and stress distributions are plotted along the central line of the specimen, i.e. the line with y=0cm, which according to the classical theory represents the neutral axis of the specimen. However, these plots show that the strains and stresses developed, although smaller from those of the line with y=5cm, are not negligible. It should be mentioned that the axial strains at point (x,y)=(0,0) are equal to about one tenth of the respective ones at point (x,y)=(0,5cm), while the transverse strains at the same points are of almost the same magnitude. The last observation indicates that, under the influence of the concentrated transverse load, the neutral axis of the beam does not coincide with the axis of symmetry of the beam and it does not pass from the centroid of the cross section. The same conclusion was drawn recently for marble beams under 3PB /12/. Finally in Figs. 12

and 13 the same quantities are shown for the upper side of the beam, i.e. along the line with y=-5cm. The influence of the concentrated load is now more evident: In the vicinity of the punch the transverse strains exceed the axial ones and, also, considerable transverse stresses of equal magnitude with the axial ones are developed. Shear stresses are also generated along the length of the beam.

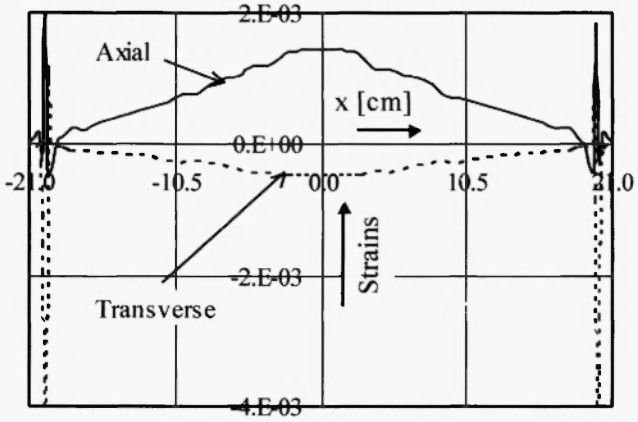

Fig.8: Axial and transverse strains along the line y=5cm.

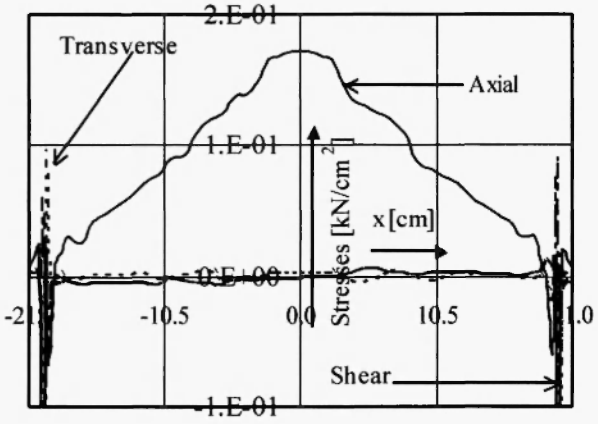

Fig. 9: The stress tensor components along the line y=5cm.

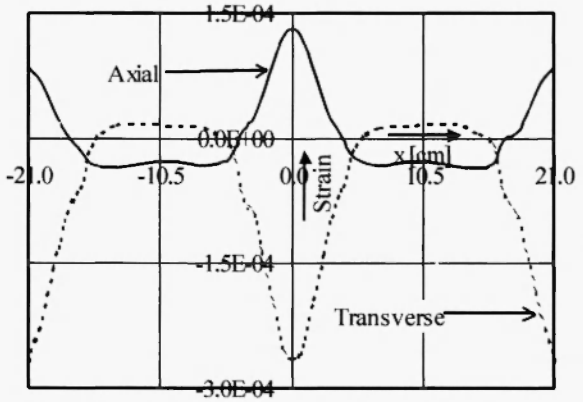

Fig. 10: Axial and transverse strains along the line y=0.

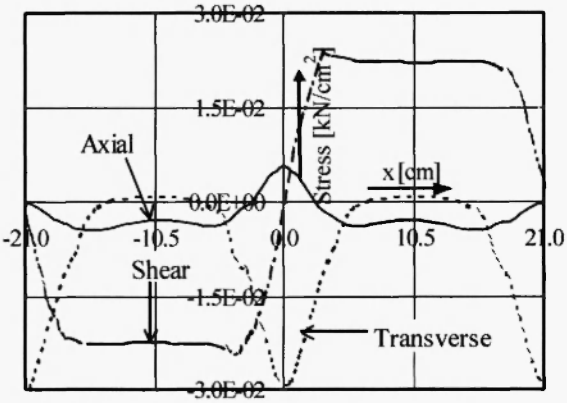

Fig. 11: The stress tensor components along the line y=0.

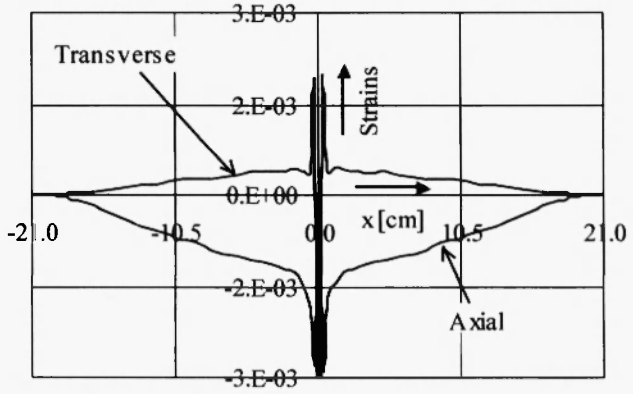

Fig. 12: Axial and transverse strains along the line y=-5cm.

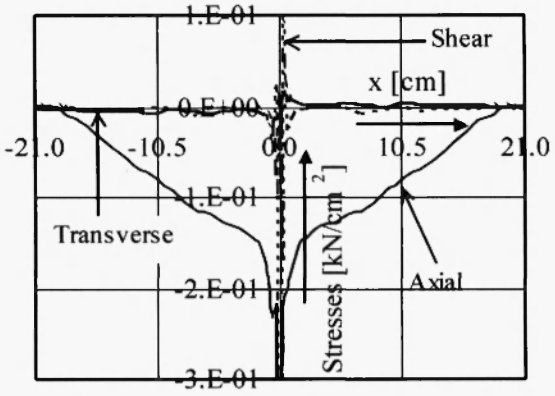

Fig. 13: The stress tensor components along the line y=-5cm.

5. DISCUSSION AND CONCLUSIONS

Comparison between theory and experiment

The results of the numerical analysis concerning the variation of the axial and transverse strains along the height of the beam are plotted in Fig.14 (continuous and dotted line, respectively) for the central section of the beam together with the respective experimental values (empty and filled symbols, respectively), for a load equal to the fracture load P=3.125 kN. Results indicate that the axial strain is not linearly distributed along the height of the beam and it is verified that the neutral axis is displaced upwards. In fact the upper half of the beam appears to be almost axial-strain free. Similar observations were made by Kourkoulis *et al.* /12/ for marble specimens. On the other hand the transverse strain reaches very high values in the immediate vicinity of the concentrated load, however the phenomenon attenuates rapidly and a constant value, equal to about one tenth of the maximum one, is reached, at a distance equal to about one fourth of the height of the beam. Axial and transverse strains are also plotted in Fig.15 for a section with x=-10 cm. Results show that the axial strain is now almost linearly distributed (although a sigmoid variation is detected exactly as it was detected recently for marble specimens of the same geometry subjected to 3PB /13/) or in other words the influence of the punch is eliminated.

In both cases the agreement between numerical results and experimental findings is very satisfactory for the longitudinal strains. Regarding the transverse strains, however, some discrepancies were observed: The experimental values are slightly but systematically smaller from the numerical ones. This is more pronounced for the section with x=-10 cm. A possible explanation of the phenomenon could be the fact that the transversely isotropic nature of the specific shellstone, ignored by the present numerical model, reinforces the beam against transverse deformation, since it acts as a horizontally laminated plate.

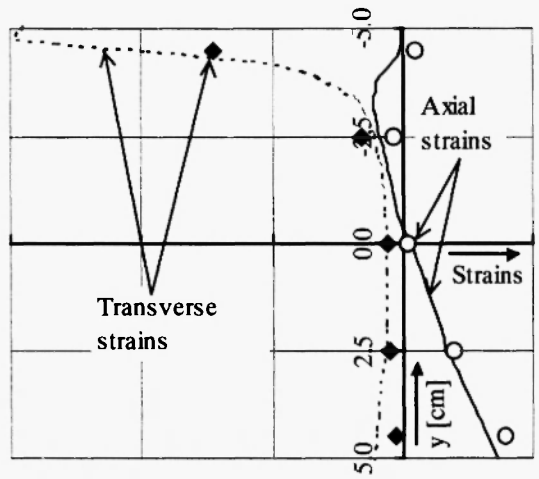

Fig. 14: Strain variation along the height of the beam at the mid-section.

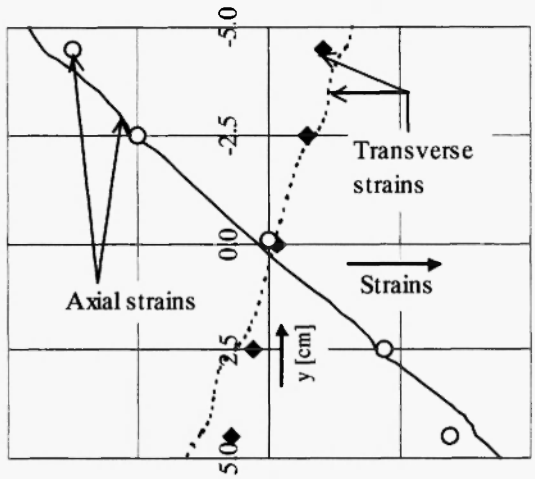

Fig. 15: Strain variation along the height of the beam at section x=-10 cm (numerically and experimentally).

Conclusions

The behaviour of shellstone prismatic beams, of small aperture (L/h=4) under 3PB was studied in this paper both numerically and experimentally. The transversely isotropic nature of the material was not taken into account; it was modeled as isotropic linearly elastic-ideally plastic. Contact elements were introduced in order to better simulate the phenomena in the immediate vicinity of the load application point. The results of the numerical analysis were compared to experimental ones from 3PB experiments.

It was concluded from this study that the classical Bernoulli-Euler technical bending theory is not adequate for the description of the problem due to the influence of the concentrated load as well as due to the small aperture of the beam. It was shown that the neutral axis of the beam does not coincide with its axis of symmetry and does not pass from its centroid. Considerable transverse and shear stresses are developed almost all over the length and height of the beam since the small aperture of the beam does not allow for the phenomena to be considered as local ones: Their influence attenuates at a distance from the point of load application equal to about half the height of the cross section of the beam. As a result the strain distribution along the height of the central section of the beam deviates completely from the assumed linear one and its upper half portion appears to be almost axial-strain free.

The numerical results approach very well the experimental findings concerning the deflection of the beam. The same is true for the axial strains, while some discrepancies are observed for the transverse ones. These may be attributed to the laminated nature of the specific material, which was not taken into account in this study. Preliminary studies with orthotropic models are encouraging, supporting this assumption.

6. REFERENCES

1. C. Wilson, "The Influence of surface loading on the flexure of beams", *Phil. Mag.*, **32**, 481-503 (1891).
2. M. Flamant, "Sur la Repartition des Pressions dans un Solide Rectangulaire Charge Transversalement", *Comptes Rendus de l' Academie des Sciences*, **114**, 1465-1468 (1892).
3. J. Boussinesq, *Comptes Rendus de l' Academie des Sciences*, **114**, 1510-1514 (1892).
4. L.N.G. Filon, *Phil. Trans.*, **201A**, 63-70 (1903).
5. V.T. Carman, *Abhandlungen Aerodynam.Inst., Techn. Hochschule*, Aachen, 7, 3 (1927).
6. F. Seewald, *Abhandlungen Aerodynam.Inst., Techn. Hochschule*, Aachen, 7, 11 (1927).
7. S. Timoshenko, *Theory of Elasticity*, Mc Graw Hill, New York, 1934.
8. I. Vardoulakis, S. Kourkoulis and C. Zambas, "Modeling of the mechanical behaviour of a conchyliates shellstone", *2nd Int. Symposium on Hard Soils Soft Rocks,* Naples, 1998; pp. 911-922.
9. MARC Analysis Research Corporation, Users' Manuals, 1995-1998.
10. Mentat 2, User's guide, 1996.
11. S. Kleftakis, Z. Agioutantis and C. Stiakakis, "Numerical simulation of the uniaxial compression test including the specimen-platen interaction", *4th Int. Coll. on Computation of Shell and Spatial Structures*, Hania, Hellas, 2000.
12. S. Kourkoulis, M. Stavropoulou, I. Vardoulakis and G. Exadaktylos, "Local strains due to punch effect in 3P bending of marble beams", *9th Int. Cong. on Rock Mech.*, Paris, 1999; pp. 623-626.
13. G. Exadaktylos, I. Vardoulakis and S.K. Kourkoulis, "Influence of nonlinearity and double elasticity on flexure of rock beams", *Int. J.of Solids and Structures*, **38**, 4119-4145 (2001).